High Pressure Research
Publication details, including instructions for authors and subscription information:
http://www.informaworld.com/smpp/title~content=t713679167

Structural stability of multiferroic $BiFeO_3$

J. L. Zhu[a]; S. M. Feng[a]; L. J. Wang[a]; C. Q. Jin[a]; X. H. Wang[b]; L. T. Li[b]; Y. C. Li[c]; X. D. Li[c]; J. Liu[c]
[a] Institute of Physics, Chinese Academy of Sciences, Beijing, People's Republic of China [b] State Key Laboratory of New Ceramics and Fine Processing, Department of Materials Science and Engineering, Tsinghua University, Beijing, People's Republic of China [c] Institute of High Energy Physics, Beijing High Pressure Research Center, Chinese Academy of Sciences, Beijing, People's Republic of China

Online publication date: 02 June 2010

To cite this Article Zhu, J. L. , Feng, S. M. , Wang, L. J. , Jin, C. Q. , Wang, X. H. , Li, L. T. , Li, Y. C. , Li, X. D. and Liu, J.(2010) 'Structural stability of multiferroic $BiFeO_3$', High Pressure Research, 30: 2, 265 — 272
To link to this Article: DOI: 10.1080/08957959.2010.493670
URL: http://dx.doi.org/10.1080/08957959.2010.493670

High Pressure Research
Vol. 30, No. 2, June 2010, 265–272

Taylor & Francis
Taylor & Francis Group

Structural stability of multiferroic $BiFeO_3$

J.L. Zhu[a]*, S.M. Feng[a], L.J. Wang[a], C.Q. Jin[a], X.H. Wang[b], L.T. Li[b], Y.C. Li[c], X.D. Li[c] and J. Liu[c]

[a]*Institute of Physics, Chinese Academy of Sciences, Beijing 100190, People's Republic of China;* [b]*State Key Laboratory of New Ceramics and Fine Processing, Department of Materials Science and Engineering, Tsinghua University, Beijing 100084, People's Republic of China;* [c]*Institute of High Energy Physics, Beijing High Pressure Research Center, Chinese Academy of Sciences, Beijing 100039, People's Republic of China*

Multiferroic $BiFeO_3$ was fabricated via a high pressure of 5 GPa at 900 °C. The crystal structure of the $BiFeO_3$ ceramic was determined by X-ray diffraction (XRD) to be a rhombohedral perovskite with a space group of $R3c$. The temperature dependence of XRDs was collected down to 5 K under ambient pressure that showed no structure phase transition. The structural evolution of $BiFeO_3$ under high pressures up to 56.6 GPa was studied at room temperature using a diamond anvil cell combined with synchrotron radiation XRD. A possible phase transition was proposed at around 10 GPa. The bulk modulus was estimated to be $B_0 = 97.3(7)$ GPa in the low-pressure range.

Keywords: multiferroics; $BiFeO_3$ perovskite; synchrotron radiation; equation of state

1. Introduction

Multiferroics, which exhibit ferroelectricity and ferromagnetism simultaneously, *i.e.* being both magnetically and electrically polarized, have stimulated a great deal of research interest during very recent years [1–5]. Besides the tremendous applications based on the mutual control of polarization and magnetization via a magnetoelectric effect, *i.e.* the induction of electric polarization by means of a magnetic field or vice versa, the fundamental physics behind it is fascinating. Unfortunately, the number of multiferroic compounds is dramatically reduced to a very few cases with respect to the coexistence of ferroelectric and ferromagnetics due to the incompatibility between magnetism and ferroelectricity in both electronic and crystal structure requirements. The $BiFeO_3$ crystal is a rare example of a single-phase room temperature multiferroic compound. The lone pair effect of Bi $6s^2$ (Pb or Tl) [6] electrons has proved to play a pivotal rule in inducing structural distortion and ferroelectricity, such as for ferroelectric $PbTiO_3$ [7] and $PbVO_3$ [8] with gigantic spontaneous polarization. Like Pb^{2+} and Bi^{3+} with $6s^2$ electrons, lone pair is the key factor in triggering ferroelectricity in perovskite multiferroic $BiFeO_3$ [9,10]. The multiferroic $BiFeO_3$ is a ferroelectric–antiferromagnet and exhibits a comparatively large magnetoelectric effect [9,10].

*Corresponding author. Email: jlzhu04@aphy.iphy.ac.cn

ISSN 0895-7959 print/ISSN 1477-2299 online

DOI: 10.1080/08957959.2010.493670
http://www.informaworld.com

Among known multiferroics, $BiFeO_3$ has the highest Neél temperature with $T_N = 643\,K$ and the highest ferroelectric Curie temperature with $T_C = 1083\,K$ [11,12]. Therefore, it attracts much attention for multiferroic studies. In the perovskite-like crystal structure of $BiFeO_3$ with space group $R3c$, the Fe^{3+} ions are in distorted oxygen octahedra, while the Bi^{3+} ions occupying the dodecahedral positions are strongly shifted from the central position towards one of the Fe^{3+} ions due to the lone pair effect [13,14]. This enhances the ferroelectricity in this compound. The antiferromagnetic order in $BiFeO_3$ is in the form of a complex incommensurate spin modulation structure [15–18]. In recent years, the structure property, lattice dynamic, magnetic behavior and spin transition of multiferroic $BiFeO_3$ have been studied under pressure using synchrotron X-ray diffraction (XRD), far-infrared spectroscopy, Raman investigation, as well as using theoretical calculations [19–26]. The preliminary results revealed that the structural evolution of $BiFeO_3$ under pressure is very interesting but complicated. It is noted that both pressure and low temperature can influence crystal structure in most cases in a similar way by shrinking the lattice. In this paper, we focus on the pressure-tuned structural stability of $BiFeO_3$ up to 56.6 GPa. We also investigated the stability of $BiFeO_3$ in the temperature range of 5–300 K under ambient pressure. We compared both effects in terms of volume change.

2. Experiments

The polycrystalline $BiFeO_3$ ceramic was fabricated under high pressures using the solid-state reaction method. A stoichiometric mixture of Bi_2O_3 (Alfa Aesar, 99.99%) and Fe_2O_3 (99%) was finely ground, palletized, and enveloped with silver foil to avoid contamination from the ambience. The ultimate synthesis was conducted in a cubic anvil-type apparatus by keeping the specimen at 900 °C and 5 GPa for 10 min. Pressure was released slowly after quenching the specimen to room temperature.

The powder XRD experiments were performed with an M18AHF diffractometer (Mac Science, Japan) employing Cu K_α radiation. Low-temperature XRD data at ambient pressure were collected with a helium liquid cooling apparatus fixed on the M18AHF diffractometer. Data processing and structure refinement were performed by employing the GSAS Le Bail package [27] combined with the Powder X software package [28].

High-pressure synchrotron XRD experiments were performed at room temperature on the 3W1A high-pressure beam-line at the Beijing Synchrotron Radiation Facility (BSRF). The diffraction patterns were recorded with white synchrotron radiation in an energy-dispersive mode. Finely ground powders of $BiFeO_3$, together with a tiny piece of ruby crystal for calibrating the inner pressure, were loaded into a sample chamber with a diameter of around 100 μm of a T301 stainless steel gasket. The gasket was pre-indented from 300 μm thickness to about 30 μm before the hole was drilled. A mixture of methanol and ethanol (4:1) was used as the pressure-transmitting medium. A high pressure was generated in the diamond anvil cell with a diamond culet size of 300 μm. The inner pressure in the chamber was monitored via the shift of the fluorescence bands of Cr^{3+} in the ruby crystal [29]. Polychromatic radiation was focussed to a spot of $30 \times 20\,\mu m^2$ in size. A solid-state germanium detector was located at a fixed angle of 7.45 ° with respect to the incident synchrotron radiation. The d spacing of different reflections ($h\,k\,l$) of $BiFeO_3$ crystal was calculated according to the Bragg law:

$$E * d = \frac{6.19925}{\sin\theta}, \tag{1}$$

where E is the beam energy.

3. Results and discussion

The XRD pattern collected on our $BiFeO_3$ sample at room temperature is shown in Figure 1. All the peaks in the pattern can be well indexed on the basis of the $R3c$ structure, in good accordance with references [13,14].

As aforementioned, applied pressure or decreasing temperature can affect the crystal structure, in terms of compressing the lattice that in turn results in changes of electronic or magnetic ordering. The physical properties of multiferroic compounds are highly sensitive to the crystal structure changes. For example, a series of magnetic ordering takes place for $RMnO_3$ upon reducing temperature [2]. XRD measurements of $BiFeO_3$ polycrystalline sample were conducted down to 5 K and no structural transition was observed. This is consistent with the physical property measurements that show the antiferromagnetic ordering of $BiFeO_3$ persisting in the low-temperature domain [13]. Figure 2 shows the evolution of lattice parameters a and c and volume V of the $BiFeO_3$ crystal with decreasing temperature. With decreasing temperature, the compressibility for $\Delta a/a$,

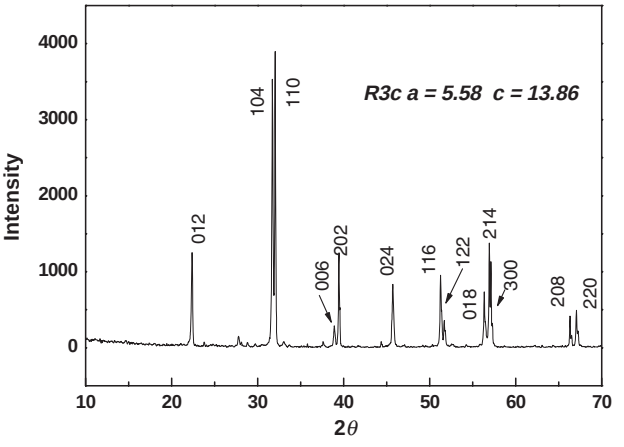

Figure 1. XRD pattern collected on the $BiFeO_3$ crystal at room temperature and ambient pressure that can be well indexed with the space group $R3c$.

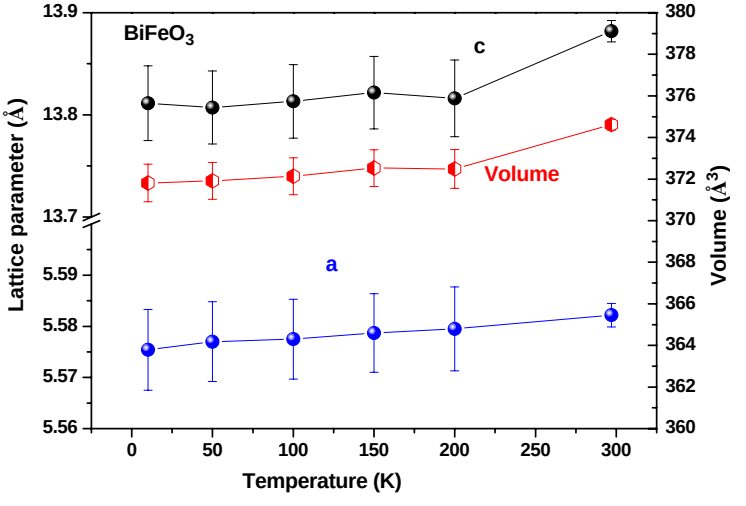

Figure 2. The evolution of lattice parameters a and c and volume V of the $BiFeO_3$ crystal with decreasing temperature.

$\Delta c/c$ and $\Delta V/V$ are 0.12%, 0.51%, and 0.75% from room temperature to 5 K, respectively. It is clear that the c-axis is softer than the a-axis.

Furthermore, the *in situ* high-pressure energy-dispersive synchrotron XRD experiments were performed for the $BiFeO_3$ polycrystalline sample at room temperature, as displayed in Figure 3. The spectra were collected at a pressure ranging between ambient pressure and 56.6 GPa. Except for the five fluorescent peaks located at 9.4, 10.9, 13.0, 15.3, and 22.1 KeV, respectively, all the other peaks can be well indexed by the $R3c$ space group. It is clear that all the diffraction peaks of $BiFeO_3$ shift to the higher energy with increasing pressure, indicating the shrinking of the lattice. Figure 4 shows the evolution of five diffraction peaks in d-space, with corresponding indices of (1 0 2), (1 1 0), (1 0 4), (2 0 2) and (2 0 4), respectively.

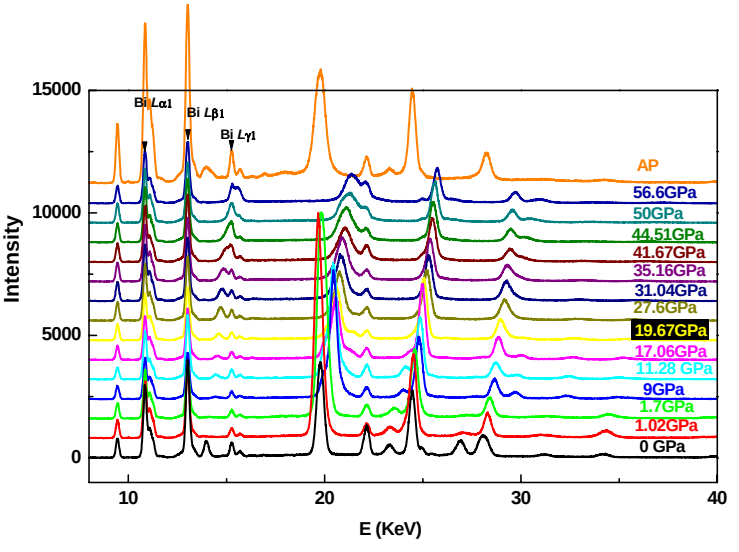

Figure 3. *In situ* high-pressure energy-dispersive XRD patterns of $BiFeO_3$ at room temperature, with pressures up to 56.6 GPa (Bi $L_{\alpha 1}$, Bi $L_{\beta 1}$ and Bi $L_{\gamma 1}$ indicate the fluorescent peaks of element Bi, respectively).

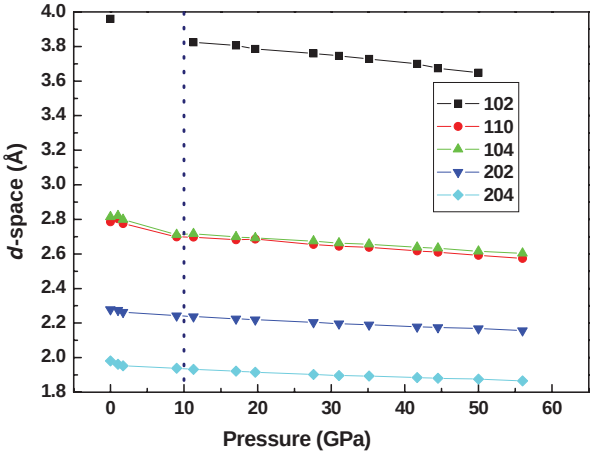

Figure 4. The evolution of five diffraction peaks in d-space with the corresponding indices of (1 0 2), (1 1 0), (1 0 4), (2 0 2) and (2 0 4), respectively.

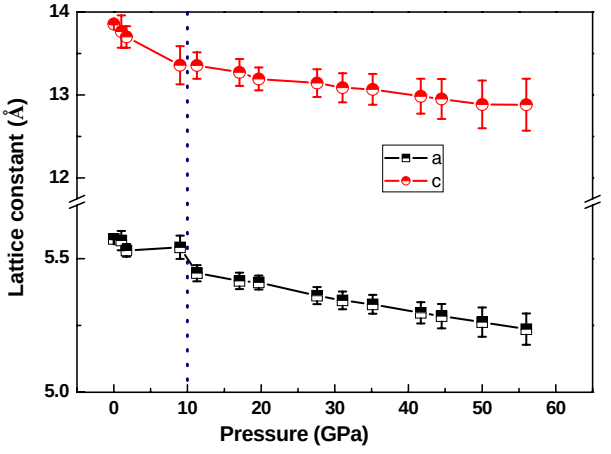

Figure 5. Pressure dependence of the lattice parameters of the $BiFeO_3$ ceramic.

Figure 5 shows the pressure dependence of the lattice parameter. Lattice parameter variations with increasing pressure were calculated through d-space values of the diffraction peaks under certain pressures. As shown in the plot, with increasing pressure of up to 56.6 GPa, the compressibility for $\Delta a/a$, $\Delta c/c$ is 6.0% and 7.0%, respectively. This means that the c-axis is a little easier to compress than the a-axis, which is consistent with the temperature evolution of the lattice parameters in $R3c$ $BiFeO_3$. Comparing with low-temperature contraction, the high-pressure effects are more profound. For example, in a simply analogy of volume change, the shrink at 5 K is comparable to the volume change at ~0.5 GPa. Low-temperature experiments down to 5 K could not provide comparable lattice shrinking effects such as high pressure experiments with a couple of tens of GPa scale, and it was only similar to very low-pressure conditions. Therefore, it does not make sense to simply link low-temperature experimental data to the results from the high-pressure experiment.

In order to obtain an evaluation of the compressibility, volume compression V/V_0 as a function of pressure is plotted in Figure 6. It is noted that although no new diffraction peaks emerge or original peaks disappear in the full pressure range, there is an obvious kink at ~10 GPa in the

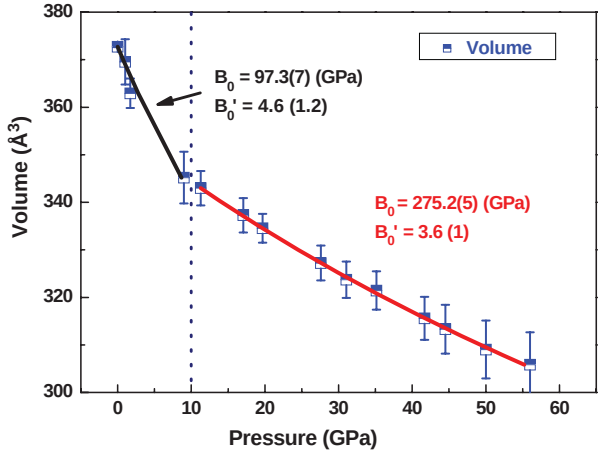

Figure 6. Pressure dependence of the volume compression of the $BiFeO_3$ ceramic.

d-space as well as in the lattice parameter/volume curves shown in Figures 5 and 6, respectively. Despite the lack of key experimental data points between 3 and 8 GPa, the well-known fact that a loss of hydrostatic conditions at around 10 GPa for methanol–ethanol mixture could contribute to the 'hard to compression' behavior for the higher pressure range. However, the difference in discontinuity in the lattice parameters a and c (in Figure 5) could be an indication of a phase transition during the compression process. This is consistent with the result in [23,26]. Further experiments using a relatively high-resolution set-up such as angle-dispersive XRD and a better pressure medium are underway to resolve this issue.

The experimental data are fitted nonlinearly with the third-order Birch–Murnaghan equation of state [30]:

$$P(\text{GPa}) = \frac{3}{2} * B_0 * \left[\left(\frac{V_0}{V}\right)^{7/3} - \left(\frac{V_0}{V}\right)^{5/3}\right] * \left\{1 - \left(3 - 3 * \frac{B_0'}{4}\right) * \left[\left(\frac{V_0}{V}\right)^{2/3} - 1\right]\right\}, \quad (2)$$

where V, V_0, B_0 and B_0' are volume at pressure P(GPa), volume at ambient pressure, bulk modulus, and derivative of B_0, respectively.

From this equation, we derived bulk modulus $B_0 = 97.3(7)$ GPa with $B_0' = 4.6(1.2)$ for the low-pressure range (<10 GPa), while $B_0 = 275.2(5)$ GPa with $B_0' = 3.6(1)$ was derived for the high-pressure range (>10 GPa). The proposed phase transition was characterized by no significant discontinuity in the evolution of the unit-cell volume with pressure, but with a kink associated with small structural changes, which may be an indication of a second-order phase transition. We noted that the ratio $c/(a * 6^{1/2})$, where $(a * 6^{1/2})$ is the primitive cubic unit cell of the perovskite structure, decreases progressively with pressure and reaches a value of 1.00097 at $P = 11.28$ GPa. Thus, at this transition pressure, the volume approaches a metrically cubic cell. To further illuminate the symmetry change with pressure, we show in Figure 7 the pressure and temperature dependence of the α angle of $BiFeO_3$ in the triangular crystal symmetry. With increasing temperature, the α angle of $BiFeO_3$ remains the same, at around 59.5 ° within the system error. However, in the pressure range, the α angle of $BiFeO_3$ increases linearly with increasing pressures up to 10 GPa. Then, the α angle stays at around 60 ° with pressures up to 56.6 GPa, indicating the trend to high symmetry space group evolution driven by pressure. Based on this pressure-tuned

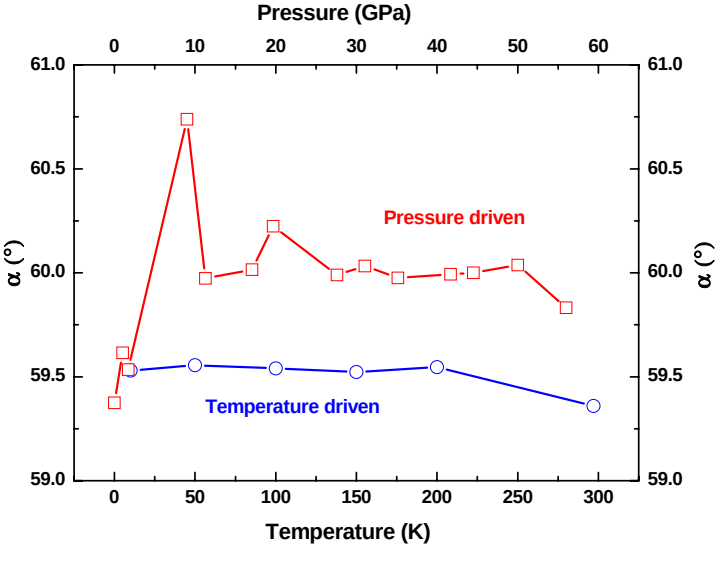

Figure 7. Pressure and temperature dependence of α angle in the triangular space group symmetry of $BiFeO_3$.

structural change, it would be interesting to further investigate the change in physical properties, such as how ferroelectricity or magnetic ordering would evolve with pressure. Such works are in progress, based on our previously designed setup [31].

4. Conclusion

A multiferroic $BiFeO_3$ ceramic with an $R3c$ space group crystal structure was synthesized under high pressures. The temperature evolution of the crystal gives no phase transition in the measured temperature range down to 5 K. The temperature and pressure evolutions of the lattice parameters show that the c-axis is more compressable than the a-axis. The bulk modulus B_0 of the $BiFeO_3$ ceramic was estimated as 97.3(7) GPa with $B_0' = 4.6(1.2)$. A possible phase transition was proposed at around 10 GPa.

Acknowledgement

This work was sponsored by the Ministry of Sciences and Technology of China.

References

[1] Z.H. Chi, C.J. Xiao, S.M. Feng, F.Y. Li, and C.Q. Jin, *Structural stability of multiferroics $BiMnO_3$ under high pressure*, J. Appl. Phys. 98, (2005), pp. 103519–103523.
[2] M. Tachibana, T. Shimoyama, H. Kawaji, T. Atake, and E. Takayama-Muromachi, *Jahn–Teller distortion and magnetic transitions in perovskite $RMnO_3$ (R=Ho, Er, Tm, Yb, and Lu)*, Phys. Rev. B 75 (2007), pp. 144425-1–5.
[3] M. Fiebig, Th. Lottermoser, D. Frohlich, A.V. Goltsev, and R.V. Pisarev, *Observation of coupled magnetic and electric domains*, Nature 419 (2002), pp. 818–820.
[4] T. Kimura, T. Goto, H. Shintani, K. Ishizaka, T. Arima, and Y. Tokura, *Magnetic control of ferroelectric polarization*, Nature 426 (2003), pp. 55–58.
[5] Th. Lottermoser, Th. Lonkai, U. Amann, D. Hohlwein, J. Ihringer, and M. Fiebig, *Magnetic phase control by an electric field*, Nature 430 (2004), pp. 541–544.
[6] N.A. Hill, *Why are there so few magnetic ferroelectrics*, J. Phys. Chem. B 104 (2000), pp. 6694–6709.
[7] R.E. Cohen, *Origin of ferroelectricity in perovskite oxides*, Nature 358 (1992), pp. 136–138.
[8] A.A. Belik, M. Azuma, T. Saito, Y. Shimakawa, and M. Takano, *Crystallographic features and tetragonal phase stability of $PbVO_3$, a new member of $PbTiO_3$ family*, Chem. Mater. 17 (2005), pp. 269–273.
[9] G.A. Smolenskii and I.E. Chupis, *Ferroelectromagnets*, Sov. Phys. Usp. 25 (1982), pp. 475–493.
[10] A.K. Zvezdin and A.P. Pyatakov, *Phase transitions and the giant magnetoelectric effect in multiferroics*, Phys. Usp. 47(4) (2004), pp. 465–470.
[11] G.A. Smolenskii, V. Yudin, E. Sher, and Yu.E. Stolypin, *Weak ferromagnetism of some $BiFeO_3$–$Pb(Fe_{0.5}Nb_{0.5})O_3$ perovskites*, Sov. Phys. – JETP 16 (1963), pp. 622–624.
[12] Y.E. Roginskaya, Y.N. Venevtsev, and G.S. Zhdanov, *Coexistence of antiferromagnetic and special dielectric properties in the $BiFeO_3$–$LaFeO_3$ system*, Sov. Phys. – JETP 17 (1963), pp. 954–955.
[13] P. Fischer, M. Polomskya, I. Sosnowska, and M. Szymanksi, *Temperature dependence of the crystal and magnetic structures of $BiFeO_3$*, J. Phys. C 13 (1980), pp. 1931–1940.
[14] J.D. Bucci, B.K. Robertson, and W.J. James, *The precision determination of the lattice parameters and the coefficients of thermal expansion of $BiFeO_3$*, J. Appl. Crystallogr. 5 (1972), pp. 187–191.
[15] I. Sosnowska, T. Peterlin-Neumaier, and E. Steichele, *Spiral magnetic ordering in bismuth ferrite*, J. Phys. C 15 (1982), pp. 4835–4846.
[16] I. Sosnowska, M. Loewenhaupt, W.I.F. David, and R. Ibberson, *Investigation of the unusual magnetic spiral arrangement in $BiFeO_3$*, Phys. B 180–181 (1992), pp. 117–118.
[17] A.V. Zalesskii, A.A. Frolov, and A.K. Zvezdin, *Effect of spatial spin modulation on the relaxation and NMR frequencies of ^{57}Fe nuclei in a ferroelectric antiferromagnet $BiFeO_3$*, JETP 95 (2002), pp. 101–105.
[18] J. Wang, J. Neaton, H. Zheng, V. Nagarajan, S.B. Ogale, B. Liu, D. Viehland, V. Vaithyanathan, D.G. Schlom, U.V. Waghmare, N.A. Spaldin, K.M. Rabe, M. Wuttig, and R. Ramesh, *Epitaxial $BiFeO_3$ multiferroic thin film heterostructures*, Science 299 (2003), pp. 1719–1722.
[19] A.G. Gavriliuk, V.V. Struzhkin, I.S. Lyubutin, M.Y. Hu, and H.K. Mao, *Phase transition with suppression of magnetism in $BiFeO_3$ at high pressure*, JETP Lett. 82 (2005), pp. 224–227.
[20] A.G. Gavriliuk, V.V. Struzhkin, I.S. Lyubutin, and I.A. Troyan, *Equation of state and structural transition at high hydrostatic pressures in the $BiFeO_3$ crystal*, JETP Lett. 86 (2007), pp. 197–201.

[21] I.S. Lyubutin, A.G. Gavriliuk, and V.V. Struzhkin, *High-spin-low-spin transition and the sequence of the phase transformations in the $BiFeO_3$ crystal at high pressures*, JETP Lett. 88 (2008), pp. 524–530.
[22] V.I. Zinenko and M.S. Pavlovski, *Lattice dynamics of $BiFeO_3$ under hydrostatic pressure*, Phys. Solid State 51 (2009), pp. 1404–1408.
[23] R. Haumont, P. Bouvier, A. Pashkin, K. Rabia, S. Frank, B. Dkhil, W.A. Crichton, C.A. Kuntscher, and J. Kreisel, *Effect of high pressure on multiferroic $BiFeO_3$*, Phys. Rev. B 79 (2009), pp. 184110-1–10.
[24] S.L. Shang, G. Sheng, Y. Wang, L.Q. Chen, and Z.K. Liu, *Elastic properties of cubic and rhombohedral $BiFeO_3$ from first-principles calculations*, Phys. Rev. B 80 (2009), pp. 052102-1–4.
[25] A.A. Belik, H. Yusa, N. Hirao, Y. Ohishi, and E.T. Muromachi, *Structural properties of multiferroic $BiFeO_3$ under hydrostatic pressure*, Chem. Mater. 21 (2009), pp. 3400–3405.
[26] Y. Yang, L.G. Bai, K. Zhu, Y.L. Liu, S. Jiang, J. Liu, J. Chen, and X.R. Xing, *High pressure Raman investigations of multiferroic $BiFeO_3$*, J. Phys.: Condens. Matter 21 (2009), pp. 385901-1–5.
[27] A.C. Larson and R.B. Von Dreele, *General structure analysis system (GSAS)*, Los Alamos National Laboratory Report LAUR, 2004, pp. 86–748.
[28] C. Dong, *PowderX: Windows-95-based program for powder X-ray diffraction data processing*, J. Appl. Crystal. 32 (1999), pp. 837–838.
[29] H.K. Mao, J.A. Xu, and P.M. Bell, *Calibration of the ruby pressure gauge to 800 kbar under quasi-hydrostatic conditions*, J. Geophys. Res. 91 (1986), pp. 4673–4676.
[30] F. Birch, *Finite elastic strain of cubic crystals*, Phys. Rev. 71 (1947), pp. 809–824.
[31] J.L. Zhu, C.Q. Jin, W.W. Cao, and X.H. Wang, *Phase transition and dielectric properties of nanograin $BaTiO_3$ ceramic under high pressure*, Appl. Phys. Lett. 92 (2008), pp. 242901-1–13.